

See discussions, stats, and author profiles for this publication at: <https://www.researchgate.net/publication/240626144>

Axinite mineral group in low-grade regionally metamorphosed rocks in southern New Zealand

Article

CITATIONS

11

READS

32

2 authors:



Ian Pringle

Broken hill prospecting

7 PUBLICATIONS 145 CITATIONS

SEE PROFILE



Y. Kawachi

University of Otago

44 PUBLICATIONS 807 CITATIONS

SEE PROFILE

Axinite mineral group in low-grade regionally metamorphosed rocks in southern New Zealand

IAN J. PRINGLE AND YOSUKE KAWACHI

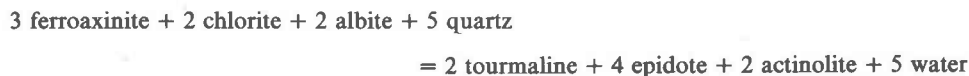
*Geology Department, University of Otago
Dunedin, New Zealand*

Abstract

In southern New Zealand, minerals of the axinite group are widespread in vein assemblages in regionally metamorphosed rocks of the prehnite–pumpellyite, pumpellyite–actinolite, and chlorite zone greenschist facies. Fe, Mg-axinites, approaching end-member ferroaxinite in composition, along with quartz and often prehnite, pumpellyite, iron-rich epidote, and chlorite fill veins in spilitized volcanic and greywacke lithologies. Tinzenite and more commonly manganaxinites occur in quartz veins in nearby ferruginous and manganese-rich cherts. Chemical analyses of vein axinites are presented, as well as analyses of four porphyroblastic ferroan manganaxinites which occur as rock-forming minerals at widely separated localities.

Compositional variability in published axinite analyses along with those of this study can be attributed partly to formation temperatures. A low-temperature miscibility gap may exist in the axinite group. Tinzenite or manganaxinite and ferroaxinite are stable in low-grade metamorphic rocks of appropriate compositions, whereas ferroan manganaxinites and manganiferous ferroaxinites occur in some pegmatites, skarns, and regionally metamorphosed rocks which equilibrated at more elevated temperatures.

For a wide range of bulk compositions in biotite and garnet zone greenschist facies and amphibolite facies rocks of southern New Zealand, tourmaline is the only observed borosilicate phase. At metamorphic conditions typical of these grades, axinite minerals would be restricted to relatively Ca-rich lithologies by a reaction of the form:

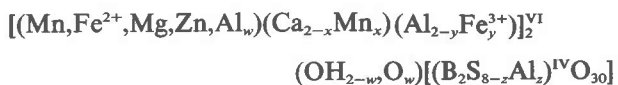


Introduction

Minerals of the axinite group have long been recognized as typical phases in manganese-ore deposits, skarns, and pegmatites and associated high-temperature environments. Ozaki (1970, 1972) examined the relationship between mode of occurrence of axinite and chemical composition. He distinguished five different categories: manganese and ferruginous ore deposits, pegmatites, contact metamorphic and metasomatic ore deposits, regionally metamorphosed rocks, and veins in igneous and sedimentary rocks. When axinite analyses from each occurrence are plotted on a Mn–Ca–Fe diagram the manganese contents of axinites in each rock type are shown to decrease in the above order, although considerable overlap is observed (Fig. 1). Ozaki interpreted this compositional

spread as being mainly due to host rock composition.

The general formula for the axinite group proposed by Lumpkin and Ribbe (1979) is:



where $w < 1$, $x < 1$, $y \ll 1$, $z \ll 1$, and VI and IV represent co-ordination of the cations. Sanero and Gottardi (1968) have clarified the nomenclature and defined the end members ferroaxinite $[\text{Fe}^{2+}\text{Ca}_2\text{Al}_2\text{BSi}_4\text{O}_{15}(\text{OH})]$ and manganaxinite $[\text{Mn}^{2+}\text{Ca}_2\text{Al}_2\text{BSi}_4\text{O}_{15}(\text{OH})]$. The name ferroaxinite is applied to those axinites with $\text{Ca} > 1.5$ and $\text{Fe} > \text{Mn}$, and manganaxinite where $\text{Ca} > 1.5$ and $\text{Mn} > \text{Fe}$. Tinzenite includes those axinites with $\text{Ca} < 1.5$ and $\text{Mn} > \text{Fe}$ which approach the empirical composition

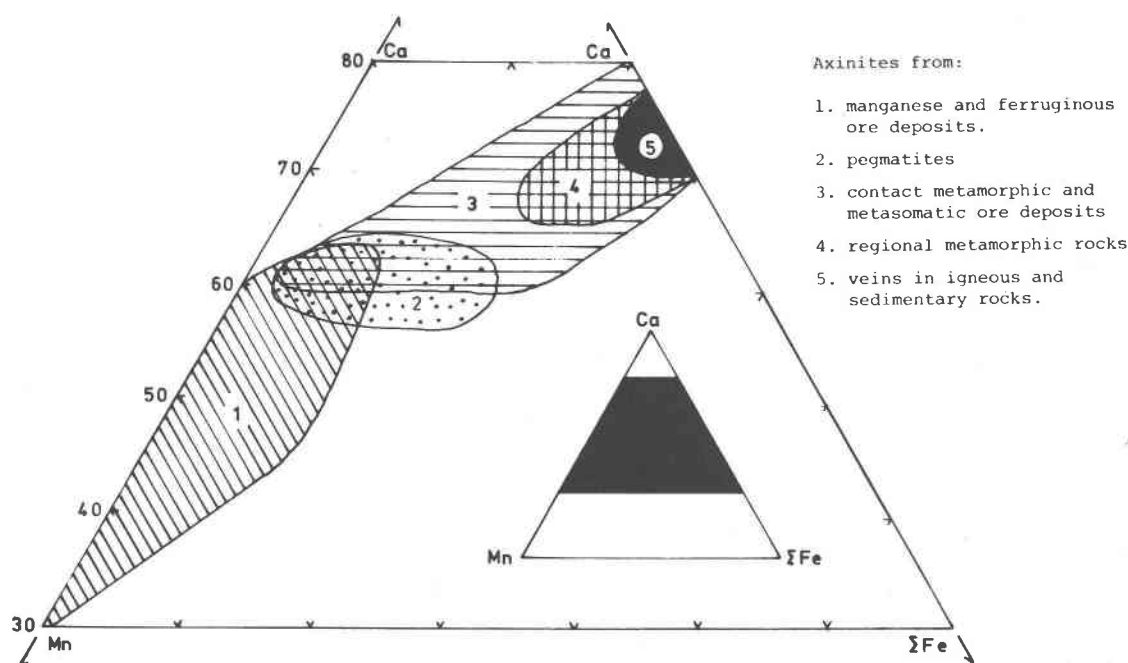


Fig. 1. Triangular Mn-Ca-Fe diagram after Ozaki (1972), showing compositional variations of axinites in different lithologies.

$\text{Mn}_2\text{CaAl}_2\text{BSi}_4\text{O}_{15}(\text{OH})$. Sanero and Gottardi (1968), followed by Ozaki (1969, 1972) and Lumpkin and Ribbe (1979), showed that substitution in the group is principally in two series, one from ferroaxinite to manganaxinite, the other from manganaxinite towards tinzenite.

Axinite in low-grade regionally metamorphosed rocks was first reported by Kojima (1944) in the Sambagawa metamorphic belt in central Japan. Here axinite occurs in a stilpnomelane-bearing band in greenschist. The only extended account of axinite as a rock-forming mineral in schists is by Nureki (1967), who described and partially analyzed manganaxinite from transitional blueschist-greenschist facies rocks of the Sangun metamorphic zone in southwest Japan, where it occurs as inclusion-studded porphyroblasts and as clear grains in nearby quartz-albite-axinite veins. The manganaxinite-bearing assemblages contain stilpnomelane + chlorite + epidote + albite + quartz \pm muscovite \pm calcite \pm sphene \pm opaque.

Examples of axinite-bearing veins in regionally metamorphic rocks are more numerous. Simonen and Wiik (1952) describe ferroaxinite-quartz-calcite veins in amphibolites and basic intrusive rocks in Finland. In a review of axinite occurrences in the Norwegian Caledonides, Carstens (1965) emphasized the association of epigenetic axinite-bearing veins with metabasite lithologies. Worldwide, over forty

records of axinite from veins in regionally metamorphosed rocks of grade higher than zeolite facies have been reported. The majority of these are in rocks containing mineral assemblages characteristic of the amphibolite facies and lower grade.

Recent workers on low-grade metamorphic rocks in southern New Zealand have recognized minerals of the axinite group at various localities in several distinct terranes (Coombs *et al.*, 1976) flanking the axis of the Haast Schist (*e.g.* Mason, 1959; Mansergh and Watters, 1970; Read and Reay, 1971; Andrews *et al.*, 1974; this study) (Fig. 2). Four occurrences are as rock-forming minerals, others are confined to veins, but all are restricted to rocks of the chlorite zone greenschist facies, pumpellyite-actinolite facies, and prehnite-pumpellyite facies. We suspect that such occurrences are relatively abundant and that minerals of the axinite group are more common in regionally metamorphosed sequences than has generally been appreciated.

Field relations and petrography

Torlesse terrane and adjacent Haast Schist terrane

These terranes consist of Late Paleozoic to Mesozoic greywackes and argillites together with rare cherts, spilitized pillow basalts, limestones and conglomerates, and their schistose derivatives. Axinite

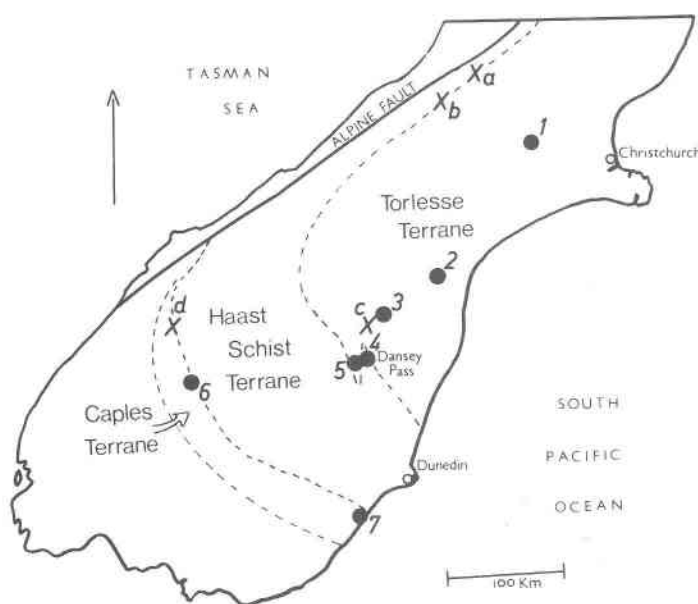


Fig. 2. Axinite localities in the southern half of the South Island, New Zealand. Crosses are locations of some previously reported axinite occurrences: (a) Lord Range (Andrews *et al.*, 1974); (b) Perth River (Mason, 1959); (c) Aviemore (Mansergh and Watters, 1970); (d) Humboldt Mountains (Bishop *et al.*, 1976). Dots are localities of analyzed axinite minerals: (1) Malvern Hills (OU 44676); (2) Lower Pareora Gorge (OU 44672); (3) Kirkliston Mountains (OU 33912); (4) Dansey Pass (Bishop, 1972) (OU 25336, 35527, 25335, 35525, 35524, 35597, 35526, 35523, 35528); (5) Hawkdun Range (Grady, 1968) (OU 21067, 21069, 21070); (6) Upper Wakatipu Area (OU 35595, 35596, 28558, 33366, 28734); (7) Akatore (Read and Reay, 1971) (OU 25686).

minerals along with other low-grade metamorphic phases occur in veins at numerous localities. Axinite porphyroblasts, however, are more restricted in distribution.

Near Dansey Pass, thick axinite-bearing quartz veins cut a schistose metachert in chlorite zone greenschist facies rocks of textural zone IIIA (Bishop, 1972). The axinite, a manganaxinite (OU 25336),¹ coexists with hematite and manganooan brunsvigite which contains 4.0–4.3 weight percent MnO. Minor tourmaline, along with spessartine and muscovite, is present in the host rock but not in the axinite-bearing veins. Elsewhere in the chlorite zone, subhedral manganaxinite porphyroblasts (OU 35528) studded with minute inclusions predominantly of quartz and hematite occur within stilpnomelane–chlorite–epidote laminae in a fine-grained hematitic metachert. Also, an impure marble contains small grains of ferroan manganaxinite (OU 25335) mantled by manganooan brunsvigite. Other phases in this rock include pris-

matic tourmaline, manganooan stilpnomelane, hematite, and abundant calcite.

At lower grade, in pumpellyite–actinolite facies rocks, veins containing quartz and pale brown manganaxinite (OU 35527) occur in massive hematitic metacherts. Pinkish brown and pale purple ferroaxinites are common constituents of anastomosing veins in nearby metabasite lithologies (OU 35523, 35524, 35525, 35526, 35597). The latter veins vary in thickness from a few mm to several cm and contain, in addition to ubiquitous quartz, variable amounts of calcite and iron-rich epidote (Ps_{26} – Ps_{28}). Iron-rich epidote is often concentrated as border zones, 1–3 cm wide in thicker ferroaxinite-bearing veins. Albite, pumpellyite, chlorite, asbestiform actinolite, sericite, pyrite, and sphene are common accessory phases. Mg-pumpellyite containing 2.5 weight percent MgO coexists with ferroaxinite in OU 35526.

Manganaxinites in veins from two other localities were analyzed. In the northern Malvern Hills, 70 km west of Christchurch, buff-brown manganaxinite (OU 44676) fills thin veinlets along with quartz in a rhodonite–pyrolusite-bearing metachert. The host

¹ Sample numbers are Geology Department, University of Otago catalogue numbers.

rock forms part of a 600-m-thick sequence of metabasites, hematitic and manganiferous metacherts, and marbles metamorphosed to prehnite-pumpellyite facies.

A large boulder of pumpellyite-bearing metachert in river gravels of Station Stream, which drains the eastern Kirkliston Mountains, contains veins up to several cm thick of quartz and yellow-brown manganaxinite (OU 33912). Red and green metacherts are important constituents in a metavolcanic sequence cropping out nearby, and probably the boulder is locally derived.

Other analyzed axinites from vein assemblages in Torlesse rocks are from the Hawkdun Range (Grady, 1968), where pale brown ferroaxinite (OU 21067, 21069, 21070) along with quartz and prehnite occupies veins cutting prehnite-pumpellyite facies metagreywackes. Axinite-bearing veins in similar lithologies have been described from the Perth River (Mason, 1959) and from near Lake Aviemore (Mansergh and Watters, 1970). These samples differ from others in this study in being remote from metabasite and/or cherty lithologies.

Porphyroblastic manganaxinites occur together with quartz, ferrostilpnomelane, minor manganian ripidolite, and sericite in a prehnite-pumpellyite facies metachert (OU 44672) from the Lower Pareora Gorge (Fig. 2). The porphyroblasts comprise six percent of the rock, are typically wedge-shaped crystals up to 300 μm diameter, and are studded with minute

inclusions of quartz and hematite which cause a pink to pale brown coloration of cores in some grains (Fig. 3).

The Torlesse rocks pass gradationally into the Haast Schist terrane with an increasing development of penetrative schistosity. Metamorphic grade in these transitional areas is commonly of pumpellyite-actinolite facies. It is near the marginal fringe of the Haast Schist terrane that axinite-bearing assemblages are widespread. Axinite has not been reported from schists of biotite zone or of higher metamorphic grades in New Zealand.

Caples terrane

The Caples Group flanking the southwestern margin of the Haast Schist terrane consists largely of volcanic arc-derived sediments with minor spilitic volcanics, limestones, and cherts. These rocks form part of the complexly deformed Te Anau Assemblage of Turnbull (1977).

Axinite-bearing quartz veins occur widely near Lake Wakatipu (e.g. Kawachi, 1975; Bishop *et al.*, 1976). Ferroaxinites from several localities were analyzed. In each case they are from veins in mafic volcanogenic rocks of prehnite-pumpellyite or pumpellyite-actinolite facies. Associated minerals, as in the ferroaxinite-bearing assemblages of the Torlesse terrane, include quartz, pumpellyite, epidote, chlorite, calcite, and albite.

A Mg-pumpellyite coexisting with ferroaxinite in

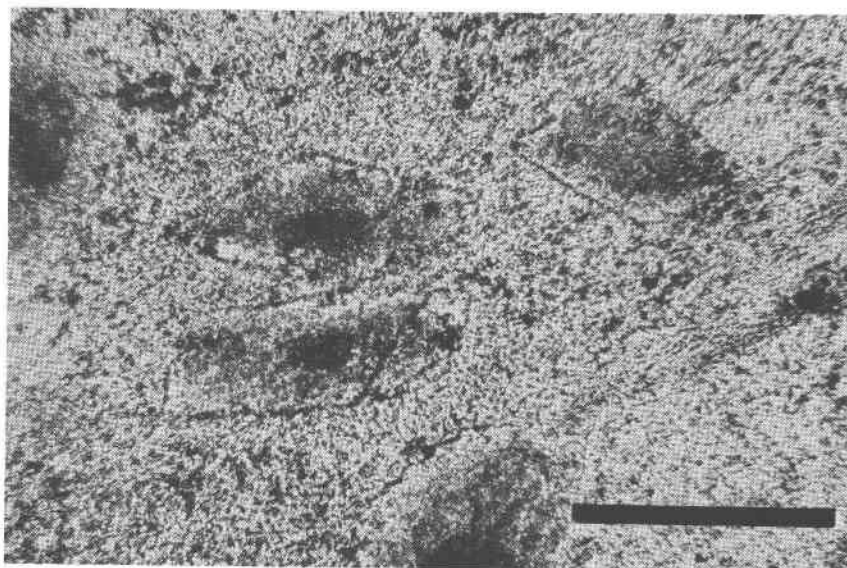


Fig. 3. Manganaxinite porphyroblasts in OU 44672. Minute inclusions of quartz and hematite are concentrated in grain cores. The fine-grained groundmass consists of quartz, ferrostilpnomelane, manganian ripidolite, and minor spessartine. Scale bar is 250 μm .

OU 28558 contains 3.1 weight percent FeO^* and 3.40 weight percent MgO , and is typical of pumpellyite compositions in rocks of the higher-grade parts of the pumpellyite-actinolite facies (Kawachi, 1975). The composition of coexisting plagioclase is almost end-member albite ($\text{Ab}_{99.1}$) and calcite in the same vein is close to pure CaCO_3 . Optical data for these phases in other ferroaxinite-bearing vein assemblages suggest similar compositions. Epidotes are all iron-rich, as indicated by their high birefringence and yellow to pale green pleochroism.

Although ferroan manganaxinite porphyroblasts occur in pale green sericitic schist (OU 33366) associated with pillowed metabasalts near Mt. Nicholas in the Thomson Mountains (Turnbull, 1974), as yet no manganaxinites have been identified in veins in this terrane. The ferroan manganaxinite porphyroblasts comprise 5.5 volume percent of the rock and are dotted with minute inclusions mainly of quartz and albite. The crystals are commonly idioblastic lozenge-shaped grains less than 200 μm in maximum dimension and are rarely twinned. Pumpellyite, along with quartz, phengite, albite, chlorite, sphene, and minor detrital epidote, completes the mineral assemblage.

Along strike to the southeast, on the coast, comparable rocks known as the Tuapeka Group also grade northwards into the Haast Schist terrane. Here, near Akatore Creek, yellowish tinzenite (OU 25686) occupies thin veinlets along with quartz, rhodonite, pyroxmangite, and apatite in an akatoreite-bearing manganiferous metachert (Read and Reay, 1971).

Mineral chemistry of tinzenite and axinites

Major elements except for boron and water have been analyzed by a JEOL JXA-5A computer-controlled electron microprobe. Analysis conditions, standards, and correction procedure are similar to those described by Nakamura and Coombs (1973).

Representative and averaged tinzenite and axinite analyses listed in order of increasing manganese content are given in Tables 1 and 2. Cationic proportions are calculated on an anhydrous and boron-free basis ($\text{O} = 28$), and water and B_2O_3 contents are estimated in stoichiometric amounts $\text{OH} = 2.0$ and $\text{B} = 2.0$. The tendency for the totals of most analyses to approach 100 percent supports the validity of this calculation. The amount of Fe_2O_3 in the analyses has been calculated on the basis of $(\text{Al}^{\text{IV}} + \text{Ti} + \text{Fe}^{3+}) = 4.000$, after assigning Al to fill tetrahedral sites where

necessary. Using this method most analyzed ferroaxinites have no or low Fe_2O_3 content (Table 2). However, for most manganaxinites Fe_2O_3 content represents a significant amount of the total iron. Likewise, wet-chemically determined compositions of manganaxinites listed by Ozaki generally have higher $\text{Fe}^{3+}:\text{Fe}^{2+}$ ratios than ferroaxinites (Ozaki, 1972). MnO contents of manganaxinites in Table 1 range from 7.19 to 16.25 weight percent and $\text{FeO} + \text{Fe}_2\text{O}_3$ ranges from 4.29 to 0.48 weight percent. Total $(\text{Fe} + \text{Mn} + \text{Mg})$ of ferroaxinites closely approaches 2.00 per formula unit and there is a negative correlation between total Fe and Mg, an opposite trend to Fe-Mg variations seen in analyzed manganaxinites (Fig. 4a). With increasing Mg content, Mn in manganese-rich phases decreases rapidly from tinzenite (Fig. 4b). Ferroaxinites, however, show limited Mg-Mn substitution, despite higher and more variable Mg content. Ferroaxinite analyses plot within a restricted field near the Ca-(Fe + Mg) join on a Ca-Mn-Fe triangular diagram (Fig. 5). They fall within the compositional range of axinites from other low-grade, regionally metamorphosed terranes (compare Fig. 1) and closely approach the ideal formula of ferroaxinite.

Tinzenite from Akatore (Table 1, 25686) contains considerably more MnO and less CaO than our analyzed manganaxinites and approaches theoretical tinzenite composition. Although magnesium contents are negligible, some of the analyses are calculated to contain up to 0.33 weight percent Fe_2O_3 . In contrast, tinzenite from Tinzens, Switzerland has 1.59 weight percent Fe_2O_3 (Milton *et al.*, 1953).

Porphyroblastic manganaxinite crystals from the Torlesse terrane in the Lower Pareora Gorge are compositionally zoned (Fig. 2), and minute quartz and hematite inclusions ($<1 \mu\text{m}$) concentrated in grain cores inhibit the quality of microprobe analyses. Typical analyses from the core and rim of a single porphyroblast are given in Table 1. For the core analysis, oxides and structural formula are recalculated assuming a 3.70 percent quartz impurity. This was estimated by reducing weight percent SiO_2 to the average value of other analyzed manganaxinites. Porphyroblast cores are enriched in MnO and depleted in total iron, Al_2O_3 , and CaO relative to porphyroblast rims. Unzoned porphyroblastic manganaxinites from Dansey Pass (OU 25335) have compositions closely similar to the cores of the Pareora mineral. Porphyroblastic manganaxinites from near Mt. Nicholas in the Caples terrane (OU 33366), although studded with quartz and albite inclusions

² FeO^* and Fe_2O_3^* will be used in this paper for total iron calculated as FeO and total iron calculated as Fe_2O_3 respectively.

Table 1. Average and selected analyses of tinzenite and manganaxinites

Specimen	tinzenite OU25686	OU25336	OU44676	OU33912	OU35527	manganaxinites			OU44672		OU33366
Number of analyses averaged	7	6	4	4	4	OU35528	OU25335	core 1	(b)	rim 1	1
SiO ₂	43.3	42.6	42.5	42.7	42.2	43.6	42.0	46.3	42.6	42.7	42.0
TiO ₂	0.02	0.07	0.03	0.05	0.01	0.00	0.04	0.17	0.18	0.01	0.11
Al ₂ O ₃	18.2	16.9	16.5	17.1	17.5	16.6	16.9	15.9	17.3	18.6	18.1
Fe ₂ O ₃ ^(a)	0.10	0.74	1.96	1.23	0.45	2.18	1.64		0.74	0.00	0.00
FeO ^(a)	0.09	0.00	0.75	0.74	0.65	0.32	2.06	2.44 ^(c)	1.99	3.19	4.29
MnO	20.6	13.12	13.12	13.14	11.72	11.37	11.31	10.53	11.44	8.78	7.19
MgO	0.08	0.30	0.19	0.14	0.30	0.46	0.62	0.18	0.20	0.33	0.56
CaO	13.3	18.9	17.6	17.9	18.8	18.3	18.6	16.4	17.8	19.5	19.2
Na ₂ O	0.03	0.03	0.02	0.03	0.02	0.03	0.02	0.04	0.04	0.01	0.05
K ₂ O	0.00	0.01	0.03	0.02	0.02	0.03	0.01	0.04	0.04	0.05	0.08
Total	95.72	92.67	92.70	93.05	91.67	92.89	93.20	92.00	92.33	93.17	91.58
B ₂ O ₃ ^(a)	6.24	6.11	6.07	6.12	6.07	6.14	6.10		6.10	6.20	6.10
H ₂ O ^(a)	1.61	1.58	1.57	1.58	1.57	1.59	1.58		1.58	1.60	1.58
Atomic proportions, O = 28											
Si	8.04	8.08	8.12	8.09	8.05	8.23	7.98		8.09	7.98	7.98
Ti	0.00	0.01	0.00	0.01	0.00	0.00	0.01		0.03	0.00	0.02
Al	3.98	3.78	3.71	3.82	3.93	3.69	3.79		3.87	4.10	4.05
Fe ³⁺	0.02	0.11	0.28	0.18	0.06	0.31	0.23		0.11	0.00	0.00
Fe ²⁺	0.01	0.00	0.12	0.12	0.10	0.05	0.33		0.32	0.50	0.68
Mn	3.24	2.11	2.12	2.11	1.89	1.82	1.82		1.84	1.39	1.16
Mg	0.02	0.09	0.05	0.04	0.09	0.13	0.18		0.06	0.09	0.16
Ca	2.65	3.84	3.60	3.63	3.84	3.70	3.79		3.63	3.90	3.91
Na	0.01	0.01	0.01	0.01	0.01	0.01	0.01		0.01	0.00	0.02
K	0.00	0.00	0.01	0.01	0.01	0.01	0.00		0.01	0.01	0.02
Total	17.97	18.03	18.02	18.02	17.98	17.95	18.14		17.97	17.98	18.00
Analyst	YK	IJP	IJP	IJP	IJP	IJP	IJP		IJP	IJP	IJP

(a) Calculated (see text).

(b) 44672 (core) recalculated assuming an excess of 3.70% SiO₂.

(c) Total Fe as FeO.

aligned subparallel to schistosity, are also compositionally unzoned. The Fe:Mn ratio of a typical analysis (Table 1, OU 33366), however, is slightly higher than Fe:Mn ratios of porphyroblastic axinites north-east of the Haast Schist axis.

In general, porphyroblastic axinite compositions are intermediate between manganaxinites and ferroaxinites from nearby metamorphic vein assemblages. This relationship is shown in Figure 5.

Mn distribution between coexisting chlorite and axinite varies consistently from negligible and minor MnO contents in chlorites from ferroaxinite-bearing

samples to several weight percent MnO in chlorites associated with manganaxinite. Ranges for phases in five samples are listed in Table 3.

Discussion

Axinite composition and metamorphic grade

In southern New Zealand the common association of Mg-pumpellyite with axinite minerals and the restricted occurrence of axinite to rocks of low metamorphic rank suggest that temperatures and pressures of axinite formation are unlikely to have

Table 2. Average and selected analyses of ferroaxinites

Specimen	OU35595	OU35525	OU21070	OU35523	OU35524	OU35596	OU35597	OU28734	OU21067	OU21069	OU35526	OU28558
Number of analyses averaged	1	1	4	4	4	3	3	7	10	4	4	7
SiO ₂	43.3	43.0	42.5	42.6	43.0	42.7	42.1	42.9	42.8	42.4	42.2	43.2
TiO ₂	0.02	0.00	0.02	0.04	0.01	0.02	0.01	0.05	0.03	0.01	0.01	0.04
Al ₂ O ₃	18.0	18.2	18.9	18.6	18.8	17.5	18.3	18.4	18.4	18.5	18.7	17.9
Fe ₂ O ₃ ^(a)	0.28	0.00	0.00	0.00	0.00	0.75	0.00	0.00	0.00	0.00	0.00	0.46
FeO ^(a)	8.37	7.25	8.33	6.87	6.15	8.24	8.96	8.91	8.78	9.26	9.61	7.55
MnO	1.95	1.58	1.51	1.27	1.26	1.25	1.11	1.08	0.98	0.72	0.59	0.46
MgO	1.15	1.97	1.19	2.55	2.91	1.39	1.33	1.50	1.36	1.20	1.21	2.40
CaO	19.6	20.1	20.0	20.2	20.1	20.0	20.3	20.0	20.1	20.1	20.1	20.1
Na ₂ O	0.02	0.02	nd	nd	nd	0.04	0.01	0.02	0.03	nd	nd	0.03
K ₂ O	0.01	0.02	nd	nd	nd	0.01	0.01	0.01	0.02	nd	nd	0.02
Total	92.70	92.14	92.45	92.13	92.23	91.90	92.13	92.87	92.50	92.19	92.42	92.16
B ₂ O ₃ ^(a)	6.21	6.21	6.20	6.22	6.26	6.14	6.11	6.23	6.21	6.17	6.18	6.22
H ₂ O ^(a)	1.61	1.61	1.61	1.61	1.62	1.59	1.59	1.61	1.61	1.60	1.60	1.61
Atomic proportions, O = 28												
Si	8.08	8.02	7.94	7.93	7.96	8.06	7.93	7.98	7.99	7.96	7.91	8.05
Ti	0.00	0.00	0.00	0.01	0.00	0.00	0.00	0.01	0.00	0.00	0.00	0.01
Al	3.96	4.00	4.16	4.08	4.10	3.89	4.06	4.04	4.05	4.09	4.13	3.93
Fe ³⁺	0.04	0.00	0.00	0.00	0.00	0.11	0.00	0.00	0.00	0.00	0.00	0.07
Fe ²⁺	1.31	1.13	1.30	1.07	0.95	1.30	1.41	1.39	1.37	1.45	1.51	1.18
Mn	0.31	0.25	0.24	0.20	0.20	0.20	0.18	0.17	0.16	0.12	0.09	0.07
Mg	0.32	0.55	0.33	0.71	0.80	0.39	0.37	0.42	0.38	0.34	0.34	0.67
Ca	3.92	4.02	4.00	4.03	3.98	4.04	4.09	3.99	4.02	4.04	4.04	4.01
Na	0.01	0.01				0.02	0.00	0.01	0.01			0.01
K	0.00	0.01				0.00	0.00	0.00	0.01			0.01
Total	17.95	17.99	17.97	18.03	17.99	18.01	18.04	18.01	17.99	18.00	18.02	18.01
Analyst	IJP	IJP	IJP	IJP	IJP	YK	YK	YK	YK, IJP	IJP	IJP	YK

(a) Calculated (see text).

nd = not determined.

exceeded the upper stability limit of Mg-pumpellyite. Recent experimental work by Schiffman and Liou (1977) and Plyusina and Ivanov (1978) have established the upper stability limit of Mg-pumpellyite to between 340° and 390°C over a *P*(fluid) range of 1 to 8 kbar. Temperatures well in excess of these undoubtedly prevailed during axinite formation in many pegmatites and skarns reported elsewhere (e.g. Mozgova, 1964).

Original locality descriptions of the analyzed axinites listed by Ozaki (1972), together with our data, reveal that the composition of axinites in regionally metamorphosed terranes varies systematically with metamorphic grade. The host lithologies of Ozaki's category 5 (Fig. 1) invariably contain mineral assemblages typical of the prehnite-pumpellyite and

pumpellyite-actinolite facies, whereas rocks of category 4 have been regionally metamorphosed to greenschist and lower amphibolite facies. Similarly, manganese and ferruginous ore deposits containing manganaxinite or tinzenite (category 1 of Ozaki, 1972) have been affected by low-grade Sambagawa metamorphism. Axinites in rocks of higher-temperature parageneses such as skarns and pegmatites are commonly ferroan manganaxinites or manganiferous ferroaxinites intermediate in composition between ferroaxinite and tinzenite end members. In general, ferroaxinite and tinzenite are stable in low-grade rocks but become more Mn- and Fe-rich respectively with increasing metamorphic grade.

This trend is compatible with our observations. Porphyroblastic manganaxinites have compositions

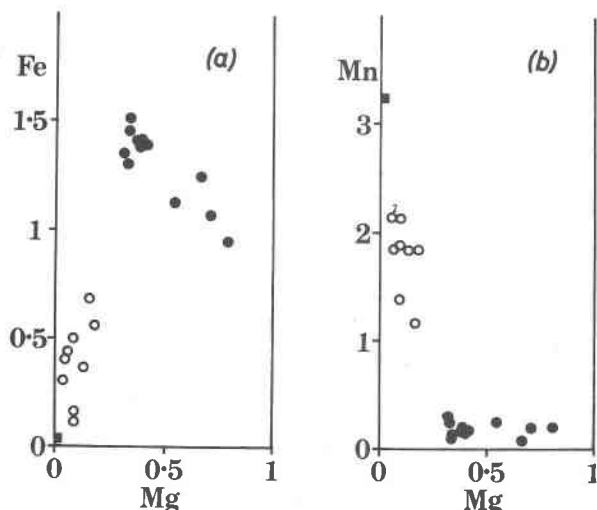


Fig. 4. Fe vs. Mg (a) and Mn vs. Mg (b) plots of representative and average tinzenite (solid square), manganaxinites (open circles), and ferroaxinites (solid circles).

intermediate between ferroaxinites and manganaxinites and tinzenites from nearby veins (Fig. 5), and it is unlikely that temperatures and pressures of axinite-bearing vein formation have surpassed those of their host rocks. Furthermore, the chemical zoning

detectable in porphyroblastic axinites in OU 44672 may reflect axinite growth accompanying increasing metamorphism. Compositions of grain cores plot near the field of vein manganaxinites on the Ca-Mn-(Fe + Mg) triangular diagram (Fig. 5). However, the distinctly FeO-, MgO-, and CaO-enriched and MnO-depleted rims of the same grains are more centrally located on the figure.

Banno and Matsui (1979, p. 68) showed that the stability temperatures of intermediate members of any mineral solid solution series depend on differences in ionic radii of substituting ions. From Banno and Matsui's data, differences in ionic radii between the divalent ions Mn, Fe, Mg, Mn, Ca suggest that in axinite a continuous solid solution between axinite and tinzenite exists only at moderately elevated temperatures typical of amphibolite facies conditions. At lower temperatures a miscibility gap in the axinite mineral series is likely to occur irrespective of bulk rock composition.

Low-temperature miscibility gaps are known to occur in other manganese-bearing minerals, such as the rhodochrosite-calcite isomorphous series (Goldsmith and Graf, 1957) and the pyralspite garnet group (Miyashiro, 1953). In both these groups the break in

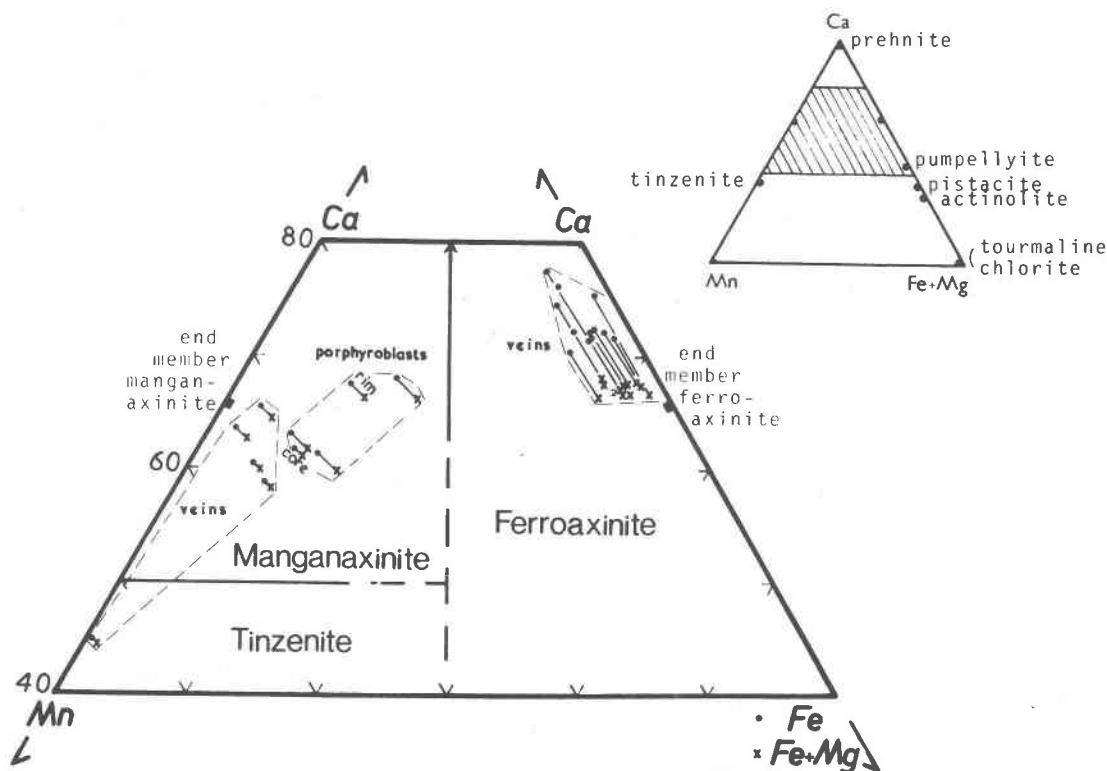


Fig. 5. Ca-Mn-Fe (Fe + Mg) triangular diagram, showing compositional variations of analyzed axinites.

Table 3. Ranges in MnO contents for coexisting axinite and chlorite

Specimen Number	MnO axinite	MnO chlorite
OU28558	0.28 - 0.85 (7)	0.05 - 0.10 (4)
OU35523	1.03 - 1.51 (4)	0.22 - 0.29 (3)
OU25335	10.45 - 12.19 (5)	2.43 - 2.92 (3)
OU44672	core 11.44 rim 8.78	2.56 - 3.02 (3)
OU25336	11.60 - 14.41 (6)	3.99 - 4.32 (3)

The number of analyses of each phase are enclosed by brackets.

solid solution disappears at high temperatures. The compositional fields of epidotes and piemontites enlarge with increasing temperatures (Miyashiro and Seki, 1958). However, in this case, the valency states of Fe and Mn (Fe^{3+} and Mn^{3+}) differ from those in axinite, and it is the Mn^{3+} content of the minerals which increases with increasing temperature.

Host rock compositional controls

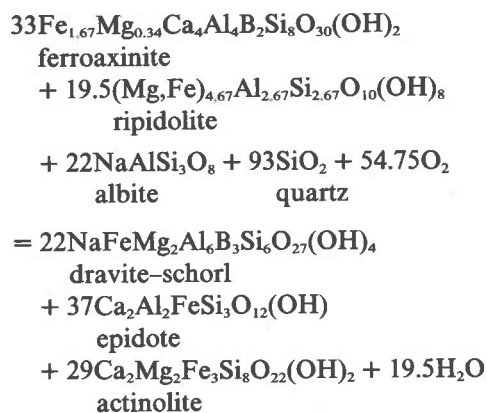
Axinite-bearing veins in low-grade, regionally metamorphosed rocks in southern New Zealand commonly cut metabasalts and associated lithologies such as metacherts, volcanogenic metasediments, or argillites. The axinites have formed in areas remote from igneous intrusion and are clearly not of contact-metamorphic paragenesis. This relationship suggests that the boron necessary for axinite formation must have been derived mainly from metabasaltic rocks or associated metacherts or argillites under the conditions of prehnite–pumpellyite, pumpellyite–actinolite, and chlorite zone greenschist facies metamorphism.

In regionally metamorphosed rocks throughout southern New Zealand tourmaline intermediate in composition between dravite and schorl [$\text{NaFeMg}_2\text{Al}_6\text{B}_3\text{Si}_6\text{O}_{27}(\text{OH},\text{F})_4$] is widespread as an accessory rock-forming phase and is locally abundant in manganiferous metacherts and marbles as well as in veins. However, in prehnite–pumpellyite, pumpellyite–actinolite, and chlorite zone greenschist facies rocks the association of tourmaline with axinite is rare. The two minerals coexist in only one sample (OU25335). In rocks metamorphosed beyond chlorite zone greenschist facies in the Haast Schist ter-

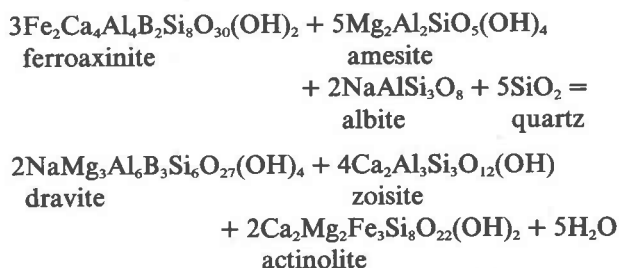
rane, tourmaline is the only boron-bearing phase recognized.

Mineral assemblages containing axinite and/or tourmaline are portrayed on ACF- B_2O_3 diagrams in Figure 6. We propose that in rocks of low metamorphic rank (chlorite zone greenschist facies and lower), the mineral assemblages epidote–axinite–chlorite and epidote–tourmaline–chlorite limit axinite and tourmaline occurrences to rocks of restricted composition (Fig. 6a). Tourmaline can occur only in relatively aluminous rocks (e.g. metapelites), whereas axinite may be present in relatively calcareous and mafic lithologies (e.g. metabasalts). Rocks with bulk-rock compositions within the area axinite–epidote–tourmaline–chlorite in Figure 6a may contain both axinite and tourmaline.

The elimination of members of the axinite group from rocks of more aluminous compositions during progressive metamorphism may be represented by equations such as:



Or, alternatively, without change in oxidation state:



Since the reactions are not univariant, due to variable MgO/FeO ratios in chlorite and amphibole phases, they may proceed over a range in temperature and pressure. Thus, in rocks with metamorphic rank equivalent to or higher than biotite zone greenschist facies, tourmaline can occur in lithologies with a wide range of compositions whereas axinite is restricted to more Ca-rich rocktypes (Fig. 6b).

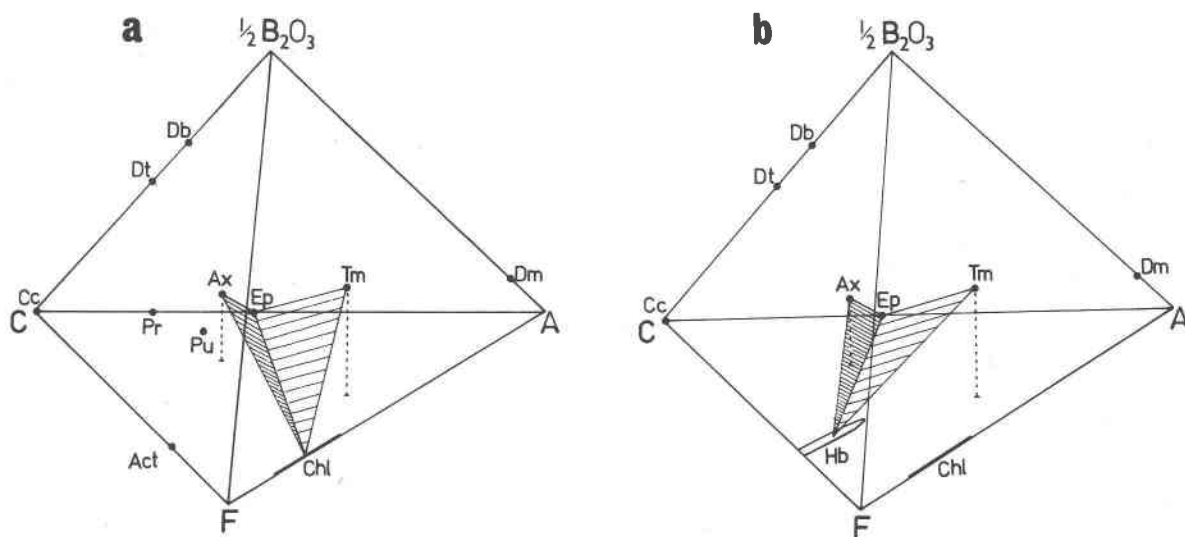


Fig. 6. ACF-B₂O₃ quaternary diagrams, assuming excess SiO₂ and H₂O are completely mobile (see text for explanation). (a) Compositional relationships between the borosilicates axinite (Ax), tourmaline (Tm), danburite (Db), datolite (Dt), and dumortierite (Dm) and metamorphic phases typical of the prehnite-pumpellyite, pumpellyite-actinolite, and chlorite zone greenschist facies. (Cc = calcite, Pr = prehnite, Pu = pumpellyite, Act = actinolite, Ep = epidote, Chl = chlorite). (b) Mineral assemblages reported in the biotite and garnet zones, greenschist facies and the amphibolite facies. Hornblende (Hb) is the stable amphibole phase. Other abbreviations as in 6a.

Within the high-grade part of the Haast Schist terrane, rock compositions appropriate for axinite formation are rare and axinite has not been reported. On the other hand, tourmaline is widespread in feldspathic and pelitic schists (e.g. Reed, 1958; Mason, 1962).

We have observed the assemblage tourmaline-calcite in marbles from the Torlesse, Caples, and Haast Schist terranes. For these rocks the interpretation of mineral assemblages on ACF-B₂O₃ diagrams cannot be applied, since SiO₂ is commonly not an excess component.

Datolite and danburite may be stable in Ca-rich lithologies, provided that sufficient boron is available. Vein assemblages consisting of datolite + calcite + quartz ± laumontite ± heulandite have been described in Torlesse greywackes from the central North Island (Manion, 1974). However, datolite and danburite have not been recorded in regionally metamorphosed rocks of southern New Zealand, and their paragenetic relationships with other metamorphic phases are unclear. Dumortierite will be restricted to very aluminous lithologies. It has been recognized in a sheared porphyritic andesite dyke at Karikari Peninsula, Northland (Black, 1973), where it is intergrown with epidote and tourmaline.

Acknowledgments

The authors thank Drs. A. Reay, M. Ozaki, I. Turnbull, and W. A. Watters for kindly providing specimens for this study, and Professor T. Sameshima for information regarding borosilicate localities in the North Island, New Zealand. Discussions on initial drafts of the manuscript by Professor D. S. Coombs and Mr. J. Y. Bradshaw led to significant improvements. Thanks also to Miss E. A. Gray (typing), Mr. J. M. Pillidge (polished thin sections), and Messrs. E. I. McKenzie and A. S. Cosgrove (microprobe maintenance).

References

- Andrews, P. G., D. G. Bishop, J. D. Bradshaw and G. Warren (1974) Geology of the Lord Range, central Southern Alps, New Zealand. *New Zealand J. Geol. Geophys.*, 17, 271-299.
- Banno, S. and Y. Matsui (1979) Thermodynamic properties of solid solutions. *Earth Science Ser.*, 4, 63-126. Iwanami Publishing Company, Tokyo.
- Bishop, D. G. (1972) Progressive metamorphism from prehnite-pumpellyite to greenschist facies in the Dansey Pass area, Otago, New Zealand. *Geol. Soc. Am. Bull.*, 83, 3177-3197.
- , J. D. Bradshaw, C. A. Landis and I. M. Turnbull (1976) Lithostratigraphy and structure of the Caples terrane of the Humboldt Mountains, New Zealand. *New Zealand J. Geol. Geophys.*, 19, 827-848.
- Black, P. M. (1973) Dumortierite from Karikari peninsula: a first record in New Zealand. *Mineral. Mag.*, 39, 245.
- Carstens, H. (1965) Axinite in the Norwegian Caledonides. *Norsk Geol. Tidsskr.*, 45, 397-415.
- Coombs, D. S., C. A. Landis, R. J. Norris, J. M. Sinton, D. J.

- Borns and D. Craw (1976) The Dun Mountain ophiolite belt, New Zealand, its tectonic setting, constitution, and origin with special reference to the southern portion. *Am. J. Sci.*, 276, 561–603.
- Goldsmith, J. R. and D. L. Graf (1957) The system CaO–MnO–CO₂: solid solution and decomposition relations. *Geochim. Cosmochim. Acta*, 11, 310–334.
- Grady, A. E. (1968) *The Metamorphic and Structural Geology of the Oturehua–Hawkdun Range area, Central Otago*. Ph.D. Thesis, University of Otago, Dunedin, New Zealand.
- Kawachi, Y. (1975) Pumpellyite–actinolite and contiguous facies metamorphism in part of the Upper Wakatipu district, South Island, New Zealand. *New Zealand J. Geol. Geophys.*, 18, 401–442.
- Kojima, G. (1944) On stilpnomelane in greenschists in Japan. *Proc. Imperial Acad. Tokyo*, 20, 322–328.
- Lumpkin, G. R. and P. H. Ribbe (1979) Chemistry and physical properties of axinites. *Am. Mineral.*, 64, 635–645.
- Manion, P. L. (1974) *The Geology of the Waimana Valley*. M.Sc. Thesis, Auckland University, Auckland, New Zealand.
- Mansergh, G. D. and W. A. Watters (1970) A note on axinite from Aviemore, Waitaki Valley. *New Zealand J. Geol. Geophys.*, 13, 725–727.
- Mason, B. (1959) Axinite from the Perth River, Westland, New Zealand. *New Zealand J. Geol. Geophys.*, 2, 137–140.
- (1962) Metamorphism in the Southern Alps of New Zealand. *Bull. Am. Museum Natural History*, 123, 211–248.
- Milton, C., F. A. Hildebrand and A. M. Sherwood (1953) The identity of tinzenite with manganoan axinite. *Am. Mineral.*, 38, 1148–1158.
- Miyashiro, A. (1953) Calcium-poor garnet in relation to metamorphism. *Geochim. Cosmochim. Acta*, 4, 179–208.
- and Y. Seki (1958) Enlargement of the composition field of epidote and piemontite with rising temperature. *Am. J. Sci.*, 256, 423–430.
- Mozgova, N. N. (1964) Axinite and datolite from polymetal skarn deposits in the Far East. *Int. Geol. Rev.*, 6, 682–689.
- Nakamura, Y. and D. S. Coombs (1973) Clinopyroxenes in the Tawhiroko dolerite at Moeraki, north-eastern Otago, New Zealand. *Contrib. Mineral. Petrol.*, 42, 213–228.
- Nureki, T. (1967) Finding of axinite-schist in the Sangun metamorphic zone at Mitaké, Yamaguchi Prefecture, southwest Japan. *J. Sci. Hiroshima Univ., Ser. C*, 5, 241–253.
- Ozaki, M. (1969) Notes on the chemical composition of axinite. *Sci. Rep. Fac. Sci. Kyushu Univ., Geol.*, 9, 129–142.
- (1970) The chemical variation of axinite in reference to their modes of occurrence. *J. Jap. Assoc. Mineral. Petrol. Econ. Geol.*, 64, 157–172.
- (1972) Chemical composition and occurrence of axinite. *Kumamoto J. Sci., Geol.*, 9, 1–34.
- Plyusina, L. P. and I. P. Ivanov (1978) *P–T* limits and fluid balance of prehnite–pumpellyite facies of metamorphism from experimental data. *Int. Geol. Rev.*, 20, 791–801.
- Read, P. B. and A. Reay (1971) Akatoreite, a new manganese silicate from eastern Otago, New Zealand. *Am. Mineral.*, 56, 416–426.
- Reed, J. J. (1958) Regional metamorphism in south-east Nelson. *N.Z. Geol. Surv. Bull.* 60.
- Sanero, E. and G. Gottardi (1968) Nomenclature and crystal chemistry of axinites. *Am. Mineral.*, 53, 1407–1411.
- Schiffman, P. and J. G. Liou (1977) Synthesis and stability relations of Mg-pumpellyite. *Proc. 2nd International Symposium on Water–Rock Interaction, Strasbourg, France*, 157–164.
- Simonen, A. and H. B. Wiik (1952) The axinites from Jokioinen and Petsamo. *Bull. Comm. Geol. Finlande*, 157, 1–6.
- Turnbull, I. M. (1974) *Geology of the Thomson Mountains, Northern Southland, New Zealand*. Ph.D. Thesis, University of Otago, Dunedin, New Zealand.
- (1977) Nomenclature in the Rangitata Geosyncline (Note). *New Zealand J. Geol. Geophys.*, 20, 803–809.

*Manuscript received, December 17, 1979;
accepted for publication, May 7, 1980.*